PHYSICAL REVIEW A **71**, 041604(R) (2005)

Bose-Einstein condensate in a box

T. P. Meyrath, F. Schreck,* J. L. Hanssen,† C.-S. Chuu, and M. G. Raizen
Center for Nonlinear Dynamics and Department of Physics, The University of Texas at Austin, Austin, Texas 78712-1081, USA
(Received 8 December 2004; published 29 April 2005)

Bose-Einstein condensates have been produced in an optical box trap. This optical trap type has strong confinement in two directions comparable to that which is possible in an optical lattice, yet produces individual condensates rather than the thousands typical of a lattice. The box trap is integrated with single-atom detection capability, paving the way for studies of quantum atom statistics.

DOI: 10.1103/PhysRevA.71.041604 PACS number(s): 03.75.−b, 32.80.Pj, 39.25.+k

The field of atom optics has now reached the stage where atom statistics are becoming a central theme following parallel developments in quantum optics where photon statistics play a crucial role. The first direct measurement of a second-order atomic correlation was reported for a beam of metastable neon [1]. In that case, a chaotic state was measured due to the high temperature of the beam. However, the situation becomes much more interesting at low temperatures where quantum statistics play a role. For example, atomic Fock states may be produced by the Mott-insulator transition [2] and with a quantum tweezer for atoms [3]. Atomic spatial antibunching should occur for a Tonks gas of bosons [4]. In a recent experiment [5], the latter was inferred from suppression of three-body loss, but was not a direct measurement of atom statistics. It is clear that these are only a few examples of an emerging theme in atom optics which is becoming increasingly important. The experiments performed to date have all relied on the use of optical lattices [5–8]. While this tool has yielded impressive results, it does not allow single-site control and addressability. Instead of a single lower-dimensional condensate, many thousands are created in parallel. For example, in the case of the Mott-insulator transition, an ideal measurement would be to turn off all sites, except one, and directly record the single-site-atom statistics. Unfortunately, this has not been possible in an optical lattice. Likewise, for the predicted quantum tweezer, a single quantum dot must be produced in order to determine the exact atomic state.

Motivated by these goals, we have developed an experimental approach presented in this Rapid Communication. This system includes an optical trap together with single-atom detection capability. Our trap consists of a crossed pair of elongated Hermite-Gaussian TEM_{01} mode beams [9]: horizontal ($hTEM_{01}$) and vertical ($vTEM_{01}$) supplemented by Gaussian beam endcaps. The geometry is illustrated pictorially in Fig. 1. With this setup we obtain trap frequencies in two dimensions which are comparable to those typically reported for optical lattices, however there is only a single condensate in one dimension. The axial motion is confined by optical endcaps, producing the textbook geometry of a "particle in a box." The resulting atomic number in this box is generally under 3500 and is controlled by evaporation timing and spacing of the endcaps [10]. Single-atom detection with nearly unit quantum efficiency has been demonstrated and is fully integrated with the new trap, paving the way for direct measurements of quantum atom statistics.

The key feature of our experiment is the optical trap. Work using Laguerre-Gaussian (LG) optical traps has produced individual one-dimensional (1D) condensates [11], but not with radial confinement sufficient for experiments of the Mott-insulator [6] or quantum-tweezer [3] sort. This geometry also is limited in trap uniformity because small waist sizes result in a short Rayleigh range which is along the axial trapping direction. Our trap geometry intrinscially overcomes this limitation due to beam orientation.

Our rubidium 87 experimental setup and method of producing TEM_{01} beams are detailed in Ref. [12]. Figure 2(a) shows a Charge-coupled device (CCD) image of the $vTEM_{01}$ beam. Both the $vTEM_{01}$ and $hTEM_{01}$ have a waist radius of 125 μm in the axial direction, which is much longer than the BEC region to provide a relatively uniform trap. Theoretical values for trap depths and oscillation frequencies are given in Table I along with comparable measured frequencies in the footnote. The measured values were obtained by fitting time-of-flight expansions to those expected for the harmonic oscillator ground states. These expansions show a change of aspect ratio indicating that the phase transition to BEC had occurred [13] with no thermal cloud observed.

The preparation of atoms in a 1D box trap consists of several steps as outlined here: (1) transfer the atoms into a

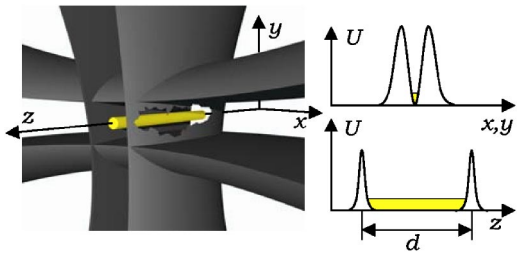

FIG. 1. The crossed TEM_{01} beams ($xTEM_{01}$) are shown pictorially on the left. The potential shapes of the trap are given in arbitrary units on the right. The potential, U, in the x and y directions have the shape of their respective TEM_{01} beams. The endcap beams produce a trap along the z axis; the Gaussian walls are separated by $d=80$ μm. The endcaps are not shown on the left; gravity is down in the pictorial.

*Present address: Institut für Quantenoptik und Quanteninformation, Innsbruck, Austria.

†Present address: National Institute of Standards and Technology, Gaithersburg, MD 20899, USA.

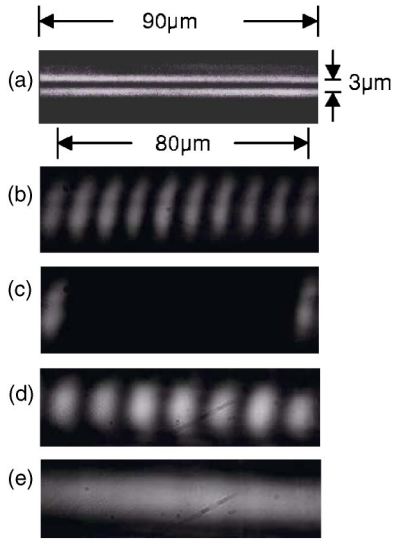

FIG. 2. Designer blue beams. Above are CCD pictures of various beams imaged as on the atom cloud. (a) $vTEM_{01}$ beam. (b) Endcap beam in a general setting showing 10 spots. (c) Endcap beam as in the $xTEM_{01}$ trap of Fig. 1. (d) Compensation beam driven with seven frequencies. (e) Compensation beam with 80 frequencies.

combined optical-magnetic trap; (2) produce a pancake-shaped BEC by evaporation while ramping off the magnetic trap; (3) transfer the BEC into the $hTEM_{01}$ trap; (4) squeeze the BEC in another direction with the elliptical red vertical trap; (5) load the elongated cloud into the $vTEM_{01}$ trap and add endcaps; (6) remove the red beams and add the compensation beam; (7) ramp up the $xTEM_{01}$ trap to full power.

The initial configuration in step (1) consists of the addition of a horizontal blue sheet of light below the atoms in the 20-Hz magnetic trap along with the vertical circular red trap ("$hTEM_{01}$, gravito-optical," and "Vert. Circular" in Table I). The blue sheet is actually a TEM_{01} mode beam which is located below the magnetically trapped atoms. The atoms are initially above the beam rather than in the node because the cloud is too large to be captured directly from the magnetic trap. The center of the magnetic trap is shifted downwards such that the atoms are pressed against the sheet and the elastic collision rate is high enough for evaporation. The magnetic trap is ramped off while the circular red beam intensity is slightly lowered to allow for radial evaporation resulting in a BEC of up to 3×10^5 atoms. Gravity presses the cloud into a pancake shape. In order to transfer the atoms into the $hTEM_{01}$ beam, an upper $hTEM_{01}$ beam is ramped on in addition to and 4-μm above the lower sheet $hTEM_{01}$ in 200 ms. This additional beam is a multiplex of the same beam ("$hTEM_{01}$, weak trap" in Table I). It surrounds the pancake-shaped BEC in the vertical direction and the lower sheet is then removed. The pancake-shaped cloud must be compressed in another direction in order to fit into the $vTEM_{01}$ beam, which is accomplished by ramping up the elliptical and ramping down the circular vertical red traps. This transfers the atoms into an elongated geometry and occurs in two 100-ms stages. With the cloud elongated, the $vTEM_{01}$ beam is ramped up in 100 ms to the weak value given in the table and the endcap beams are added, spaced 80-μm apart along the z axis. The red trap is ramped off and

TABLE I. Beams and parameters for the optical trap.

Beam[a]	$w_{x,y}(\mu m)$[b]	$w_z(\mu m)$[c]	P[d] (W)	$\omega/2\pi$[e] (kHz)	$U_0/k_B(\mu K)$[f]
$hTEM_{01}$ (Blue)	2.4	125			
gravito-optical			0.165	0.85	15
weak trap			0.165	8.3	15
trap, evap.			0.1	6.5	9.3
full trap			1.0	21	93
$vTEM_{01}$ (Blue)	1.8	125			
weak trap			0.74	27	92
full trap			3.7	61	460
End-cap (Blue)	6.1	2.5	0.011		28
Compensation (Blue)	9.8	7.2	0.001		0.54
Vert. Circular[g] (Red)	50	50	0.021	0.056	0.8
Vert. Elliptical[g] (Red)	10	125	0.085	0.8	6.6

[a]The blue beams are at 532 nm, and the red beams are at 1064 nm, which produce repulsive and attractive potentials, respectively [14].
[b]Measured radial beam waist, x for vertical and y for horizontal beams.
[c]Measured beam waist in axial direction.
[d]Measured beam power.
[e]Calculated trap frequency in the radial direction. Measured values for full $hTEM_{01}$ and $vTEM_{01}$ are 24 ± 4 kHz and 66 ± 7 kHz.
[f]Calculated peak potential height/depth divided by the Boltzmann constant [14].
[g]"Circular" and "Elliptical" refer to the shape of the intensity profile of the beam, not the polarization. All beams here are linearly polarized.

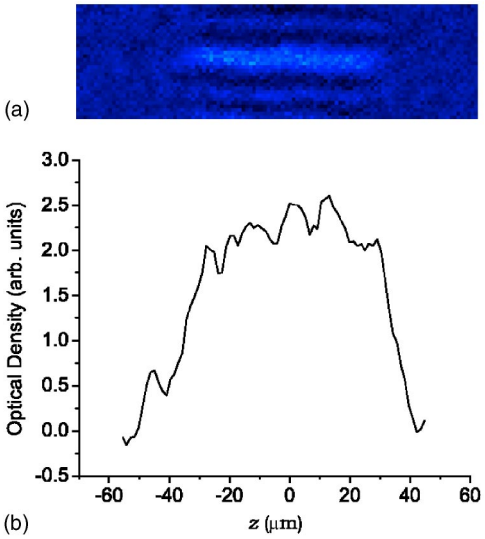

FIG. 3. (a) An absorption image of a BEC of 3×10^3 atoms in a box with Gaussian walls spaced by 80 μm along the z axis. (b) The profile of the BEC along the z axis integrated vertically. The image is *in situ*, where the absorption beam is turned on in addition to the optical trap. Resolution is limited by expansion during the 30-μs exposure and the upper and lower stripes are imaging artifacts.

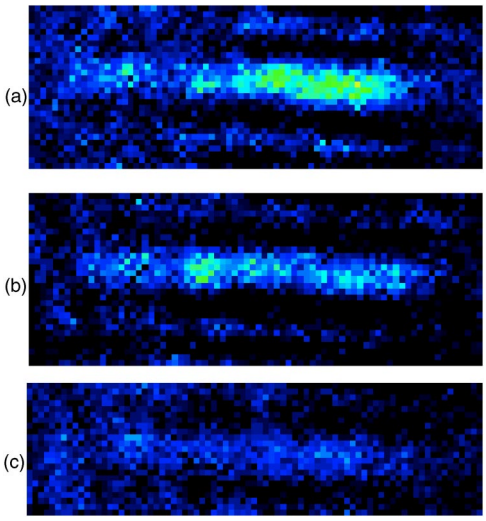

FIG. 4. Absorption images of BECs in 80-μm boxes. (a) $N\approx2\times10^3$ without a compensation beam. The cloud shows a region of higher density to the right. (b) The same as (a) but with the addition of an appropriate compensation beam. (c) $N\approx5\times10^2$ with a compensation beam averaged over 10 separate exposures. The color scale is different from that in Fig. 3.

the compensation beam ramped on. This beam is used to improve the smoothness of the axial potential giving it a boxlike shape. The atoms are now in the weak $xTEM_{01}$ box, that is, the atoms sit in a potential such that on axis there are Gaussian walls spaced by 80 μm with radial harmonic confinement of order 15-kHz geometric mean trap frequency. In order to reach the desired final number in the range of order 10^4 to 10^2, the cloud is further evaporated through the $hTEM_{01}$ trap for up to 50 ms ("$hTEM_{01}$, trap, evap." in Table I). Finally, the $vTEM_{01}$ and $hTEM_{01}$ beams are ramped to the full value ("full trap" in Table I) producing a mean radial trap frequency of order 40 kHz. An absorption image of a BEC produced in this fashion is shown in Fig. 3.

As mentioned earlier, the $hTEM_{01}$ beam multiplex, the endcap beams, and the compensation beam have a similar construction. The basic idea is to use a multiple frequency acousto-optical modulator (AOM). This AOM is driven with n distinct radio frequencies of the form: $V_{RF}=\Sigma_{i=1}^{n}A_i\cos(\omega_i t)$, where the amplitudes, A_i, and frequencies, ω_i, are independently controlled in the experiment. Each frequency produces a first-order spot [15]. For the $hTEM_{01}$ beam, these frequencies are produced by separate digital rf synthesizers and combined with a rf power combiner.

Figure 2(b) shows a CCD image of the endcap beam in a general setting. Here the AOM is driven with $n=10$ independent frequencies chosen to give an equally spaced nine-site lattice. This image demonstrates the capacity of this beam where a pair of spots may be used to form an optical quantum dot inside the cloud. In the case of this demonstration experiment, only a pair of spots ($n=2$) are used, spaced by 80 μm as the endcaps shown in Fig. 2(c). Because the rf frequencies for this beam are generated by separate stable voltage controlled oscillators each with an individual rf attenuator, the number of spots, their intensities, and their positions may be controlled independently on the 10-μs time scale.

Although the $xTEM_{01}$ trap is of good quality, it does suffer from the problem of irregular axial potential variations of order 1 $\mu K\times k_B$. This is most likely due to scattering from the holographic plate used to produce the TEM_{01} beams and other imperfect optics. This irregularity is observed to break the cloud into small sections, a phenomenon that was also observed in atom chip experiments [16]. In either case, this is due to potential variations on the order of the BEC chemical potential. A compensation beam is used to fill in valleys in the axial potential. This beam is also generated by a multiple frequency AOM, but rather than driving it with separate rf sources, a single arbitrary function generator is used to produce a stable frequency comb which results in an array of spots. Figure 2(d) shows the compensation beam driven with $n=7$ different frequencies. Because the number of spots and their intensities are arbitrary, it is possible in principle to create a beam with any intensity profile. Figure 2(e) shows the compensation beam with $n=80$ driving frequencies. The size of the structures which may be added to the profile is limited by the spot size of the beam (as in Table I). The closeness of spacing between the frequencies is limited by the possibility of parametric heating of the atoms in the optical trap. This is due to beating of the neighboring spots at their difference frequencies. Here, we operate at a minimum difference frequency of 500 kHz, which is order 10× the trap frequencies. Figure 4 shows the effects of compensation. An uncompensated condensate shows a larger density on the right in image (a). This variation can be reduced with the compensation beam, as shown in Fig. 4(b). The result is a cloud of greater uniformity but still with some irregularities on a finer scale. This level of compensation allows our optical trap to produce condensates of a much smaller number as shown in Fig. 4(c), where, with a better optimized compen-

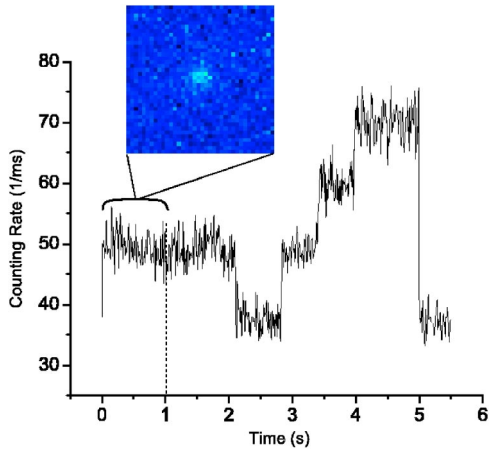

FIG. 5. Fluorescence signal for an atom transferred from the optical trap into the small MOT at time zero. The signal shows that a single initial atom is transferred and held for 2 s. The level changes afterwards are due to random loss and background loading. The inset is a fluorescence image of the single atom for a 1-s exposure from the beginning of this run.

sation profile, additional evaporation has reduced the atom number to 5×10^2. The cloud is relatively uniform, which is not possible without compensation. The small atom numbers are cross-checked with a single-atom counting system [17,18] which allows for independent verification of atom number. Our atom counting setup has been integrated as to allow for atoms to be transferred from the optical trap into a small magneto-optical trap (MOT) so they may be accurately counted by fluorescence. Figure 5 shows the signal of a single atom from the optical trap. The quantized steps illustrate the capacity to determine few atom numbers from the optical trap exactly. The level change in the signal beyond several seconds is due to background loading and loss. It should be emphasized that the single atom which was initially in the dipole trap was not extracted deterministically and serves only as a demonstration shot for the integrated detection system.

A BEC of the sort in Fig. 4(c) is a possible initial condition for further extraction experiments such as the quantum tweezer for atoms as proposed in Ref. [3], where the optical quantum dot may be produced with the additional beams in Fig. 2(b). This BEC is an ideal reservoir for single-atom extraction because the mean-field splitting in the dot is of similar order to the chemical potential of the condensate. Uniformity of the potential is currently limited by the spot size of the compensation beam and the quality of the absorption images used for the optimization. With improvements here, it should be possible to obtain a cloud in the appropriate conditions to directly study small-scale Mott-insulator physics [6] at the single well level and the Tonks-Girardeau (TG) regime. The cloud may be characterized by the interaction parameter $\gamma=mg_{1D}L/\hbar^2N$, where m is the atomic mass [5,19]. The case of $\gamma\ll1$ represents the mean-field (MF) regime whereas $\gamma\gg1$ is a TG gas. As calculated for our results, we have $\gamma\approx0.08$ for Fig. 3 which is clearly MF, however for Fig. 4(c) $\gamma\approx0.5$ and for the smallest observed condensate in our system thus far $(N\approx2.5\times10^2)$, $\gamma\approx1$ anticipating a borderline MF-TG regime. With a further flattened axial potential, it should be possible to reduce the number density and push the cloud into the TG area where it may be possible to directly study this state. This trapping geometry has the potential for further interrogation of these systems.

The authors would like to acknowledge support from the NSF, the R. A. Welch Foundation, discussions with A. M. Dudarev, and comments of B. Gutiérrez and G. Price. T.P.M. acknowledges additional support from the NSF and F.S. from the Alexander von Humboldt Foundation.

[1] M. Yasuda and F. Shimizu, Phys. Rev. Lett. **77**, 3090 (1996).
[2] D. Jacksch, Phys. Rev. Lett. **82**, 1975 (1999).
[3] R. Diener, B. Wo, M. Raizen, and Q. Niu, Phys. Rev. Lett. **89**, 070401 (2002).
[4] K. Kheruntsyan *et al.*, Phys. Rev. Lett. **91**, 040403 (2003).
[5] B. Paredes *et al.*, Nature (London) **429**, 277 (2004).
[6] M. Greiner *et al.*, Nature (London) **415**, 39 (2002).
[7] T. Kinoshita *et al.*, Science **305**, 1125 (2004).
[8] L. Tolra *et al.*, Phys. Rev. Lett. **92**, 190401 (2004).
[9] B. Seleh and M. Teich, *Fundamentals of Photonics* (Wiley, New York, 1991).
[10] A BEC is lower dimensional when $\mu_{3D}\lesssim\hbar\omega_t$, where μ_{3D} is the three-dimensional (3D) chemical potential and ω_t is the trapping frequency in the strongly confined direction(s) [13,19]. This reduces the coupling parameter to $g_{1D}=2a_s\hbar\omega_\rho$, where $a_s\cong5.3$ nm is the *s*-wave scattering length and ω_ρ is the geometric mean trap frequency in the strong directions. In the Thomas-Fermi limit, the chemical potential is $\mu_{1D}=g_{1D}N/L$, where N is the atom number and L is the condensate length. The maximum number of atoms in an effective 1D condensate, $N_{max}=L/4a_s$, depends on the length of the trap rather than the strength of transverse confinement, which is $\cong3500$ for us. Increased radial trap strength gives higher μ_{1D}, for experiments of the Mott-insulator [6] or quantum-tweezer [3] sort, for ^{87}Rb as high as 30 kHz is required, which is met by our optical trap.
[11] K. Bongs *et al.*, Phys. Rev. A **63**, 031602 (2001).
[12] T. Meyrath *et al.*, Opt. Express **13**, 2843 (2005).
[13] A. Görlitz *et al.*, Phys. Rev. Lett. **87**, 130402 (2001).
[14] R. Grimm, M. Weidemüller, and Y. Ovchinnikov, Adv. At., Mol., Opt. Phys. **42**, 95 (2000).
[15] A. Yariv and P. Yeh, *Optical Waves in Crystals* (Wiley, New York, 1984).
[16] A. Leanhardt *et al.*, Phys. Rev. Lett. **90**, 100404 (2003).
[17] D. Haubrich *et al.*, Europhys. Lett. **34**, 663 (1996).
[18] W. Alt, Optik **113**, 142 (2002).
[19] D. Petrov, G. Shlyapnikov, and J. Walraven, Phys. Rev. Lett. **85**, 3745 (2000).